4ICEGE Thessaloniki-GREECE 2007

4th International Conference on
Earthquake Geotechnical Engineering
June 25-28, 2007
Paper No. 1443

USE OF A NEW BOUNDING SURFACE MODEL FOR THE ANALYSIS OF EARTHQUAKE-INDUCED LIQUEFACTION PHENOMENA

Konstantinos ANDRIANOPOULOS[1], Achilleas PAPADIMITRIOU [2]
George BOUCKOVALAS[3]

ABSTRACT

A new numerical methodology is presented for the simulation of the non cohesive soil response under small, medium and large cyclic shear strains, with special interest given to liquefaction phenomena. The new methodology is based on a recently proposed elastoplastic bounding surface model, which has been implemented to the finite difference code *FLAC*, via its User-Defined-Model capability. The new methodology is calibrated on the basis of element laboratory tests on Nevada sand, while the simulation of centrifuge model tests from the VELACS project validates its applicability to boundary value problems. In particular, the emphasis in this paper is on comparing measurements to numerical results for the seismic response of a liquefiable sand layer that is either horizontal or has a mild slope leading to the detrimental phenomenon of lateral spreading. It is shown that the new methodology is capable of accurately predicting the time-histories of ground acceleration, excess pore pressure buildup and accumulation of displacements at all depths within the liquefiable layer. Moreover, the new methodology provides insight to the physical mechanism of accumulation of lateral displacement during lateral spreading.

Keywords: constitutive relations, bounding surface, plasticity, liquefaction, lateral spreading

INTRODUCTION

The simulation of soil response during a strong earthquake is still a subject of significant research in the field of Earthquake Geotechnical Engineering. The bulk of this research is performed via numerical analysis, which can deal with complicated situations where simple analytical solutions are too crude. The very large majority of currently available constitutive models implemented in commercial boundary value problem codes oriented towards Geotechnical Engineering are not able to quantitatively capture this response and this is mainly due to its complicated nature. In particular, features of this response like the accumulation of permanent deformations, the generation of excess pore pressures, the degradation of deformation moduli, the increase of hysteretic damping and the evolution of soil fabric as a function of the imposed cyclic shear straining require advanced constitutive modeling (e.g. Papadimitriou & Bouckovalas 2002, Elgamal et al. 2002, Dafalias & Manzari 2004), which may prove extremely difficult to implement in commercial codes. Hence, most often the solution to this problem is given via in-house codes, which are developed in various research institutes and universities and are not readily available to the technical community and have sometimes a narrow range of applicability.

This paper presents the implementation and validation of a new constitutive model for cyclic shearing in the finite difference code *FLAC* (Itasca, 1998). This model takes advantage of the UDM (User-

[1] Post-Doctoral Researcher, School of Civil Engineering, National Technical University of Athens, Greece, Email: kandrian@tee.gr
[2] Lecturer, Department of Civil Engineering, University of Thessaly, Greece
[3] Professor, School of Civil Engineering, National Technical University of Athens, Greece

Defined Model) capability of this code and has been developed with the goal to overcome the foregoing shortcomings. It is based on incremental elasto-plasticity and aims at performing realistic fully coupled dynamic analyses for practical problems of Earthquake Geotechnical Engineering.

PLASTICITY MODEL AND IMPLEMENTATION TO FLAC

The new UDM (Andrianopoulos, 2006) is a bounding surface model with a vanished elastic region that incorporates the framework of Critical State Soil Mechanics. It is based on a recently proposed model (Papadimitriou et al., 2001; Papadimitriou & Bouckovalas, 2002), which was developed with the ambition to simulate the cyclic behavior of non-cohesive soils (sands and silts), under any (small-medium-large) cyclic shear strain amplitude using a single (sand-specific) set of constants, irrespective of the initial stress and density conditions. Extensive comparison with laboratory element test results has shown that this goal has been satisfactorily achieved, since many basic aspects of cyclic soil behavior, such as the generation of excess pore pressures towards liquefaction, permanent deformations, shear-induced dilation, softening and the effects of evolving fabric anisotropy are well simulated.

In its current form, the model incorporates three (3) open cone-type surfaces with apex at the origin of stress space: (i) the Critical State surface at which deformation develops for fixed stresses and zero volumetric strain, (ii) the Bounding surface which locates the (ever-current) peak stress ratio states and (iii) the Dilatancy surface which dictates the sign of the plastic volumetric strain rate during loading. Figure 1 presents the shape of these surfaces in the triaxial [q-p] space

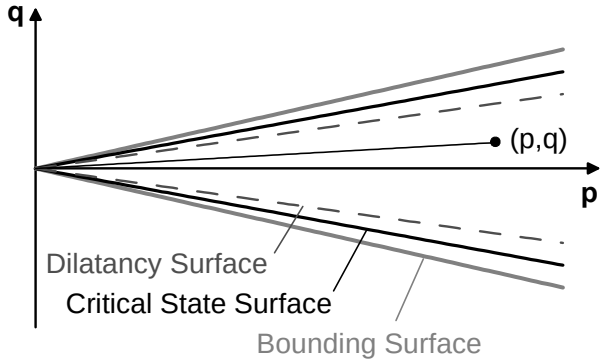

Figure 1. Model surfaces in the triaxial q-p space

Its basic feature is the direct association of shear behavior to the state parameter ψ (Been and Jefferies, 1985), which is defined, as:

$$\psi = e - e_{cs} \tag{1}$$

where e is the ever-current void ratio and e_{cs} is the void ratio on the user-defined unique critical state line (CSL) or steady state line at the ever-current mean effective stress p. In particular, this is accomplished by introducing ψ explicitly in constitutive equations, i.e. by correlating the 'opening' of the Bounding and the Dilatancy surfaces to the ever-current value of the state parameter ψ, an idea first proposed by Manzari & Dafalias (1997).

The non-linear soil response under small to medium cyclic strain amplitudes is simulated mainly by introducing a Ramberg-Osgood-type hysteretic formulation. At larger cyclic strain amplitudes elastoplasticity governs the behavior and a properly defined scalar-valued variable is introduced, which reflects macroscopically the effect of fabric evolution during shearing on the plastic modulus.

Note that there is no purely elastic region and thus the response of soil during loading is continuously elastoplastic, i.e. irrecoverable deformations occur at every incremental step. The choice of a vanished elastic region provides a smoother transition from smaller to larger strains and hence improves the numerical robustness and efficiency of the code (Naylor, 1985; Andrianopoulos, 2006). In this way, it was made possible to alleviate a number of issues that would significantly increase the required computational effort, i.e. the stress point crossing of the yield surface, the drift correction resulting from the weak enforcement of the consistency condition, and the subsequent sub-stepping in the integration scheme. The adoption of a vanished elastic region differentiates the proposed model from the original of Papadimitriou & Bouckovalas (2002) and leads to a number of other modifications as well, namely: (i) the introduction of a new mapping rule (Andrianopoulos et al., 2005) and (ii) modification of the existing interpolation rule. However, the basic constitutive equations of the original model were preserved, so that the reader can readily refer to the respective publications for more details.

In the current work, the sub-stepping technique with automatic error control proposed by Sloan et al. (2001) was adopted, which belongs to the family of effective explicit algorithms. In brief, this algorithm divides automatically the applied strain increment into sub-increments, using an estimate of the local error and attempts to control the global integration error in the computed stresses. It uses a modified Euler scheme, which consists of two basic steps. Namely, in the first step, an approximate stress increment $\Delta\sigma_1$ is calculated by using the initial matrix of elastoplastic moduli D_{ep}. In the second step, the matrix of elastoplastic moduli D_{ep} is temporarily updated and a new approximation of the stress increment $\Delta\sigma_2$ is calculated. Next, the relative error between these two approximations is estimated and, if required, sub-stepping is activated. The size of each sub-step is continuously updated so that the relative error is less than a specified tolerance level. At the end of each successful sub-step, the stress increment $\Delta\sigma_n$ is computed as the average of $\Delta\sigma_1$ and $\Delta\sigma_2$ and similar averaging is used for the hardening parameters. Further details can be found in Andrianopoulos et al. (2006b)

For the coupling of fluid-mechanical response and hence the performance of fully-coupled dynamic analyses, the process proposed in *FLAC* is adopted. Namely, the framework of quasi-static Biot theory is applied, while diffusion is controlled by single-phase Darcy equations (Itasca, 1998)

CALIBRATION OF NEW CONSTITUTIVE MODEL

In the present study, the model constants have been calibrated on the basis of data from element laboratory tests performed on fine Nevada sand at relative densities of D_r = 40 & 60% and initial effective stresses between 40 and 160 kPa (Arulmoli et al., 1992). In particular, the laboratory data originate from resonant column tests as well as direct simple shear and triaxial tests. Thus, they offer a quantitative description of various aspects of non-cohesive soil response under cyclic loading, such as shear-modulus degradation and damping increase with cyclic shear strain, liquefaction resistance and cyclic mobility. Results from this calibration process are presented in Figures 2 through 6.

Namely, Figure 2 presents a one-to-one comparison of the model simulation to the respective data for a typical undrained simple shear test at D_r = 40% and initial effective stress σ'_{vo} = 80 kPa. Similarly, Figure 3 presents a one-to-one comparison for a typical cyclic undrained simple shear test at D_r = 40% and initial effective stress σ'_{vo} = 80 kPa, where significant excess pore pressures develop leading to liquefaction.

Given that such one-to-one comparisons for *selected* monotonic and cyclic loading element tests comprise the usual way of validating constitutive models, the satisfactory comparison of Figures 2 and 3 poses as an index for a successful calibration of the model. Nevertheless, as described in detail in Papadimitriou et al (2001), for the simulation of boundary value problems where the problem of earthquake loading is at hand, it is important that a constitutive model simulates the response at any cyclic shear strain γ_{cyc} level, since the various regions of the mesh of a boundary value problem analysis do not all reach the γ_{cyc} levels of a few percent shown in Figure 3. Hence, Figure 4 presents

the overall comparison of simulations to data for cyclic shearing under small and medium γ_{cyc} amplitudes measured in the resonant column device. In particular, the comparison is made in terms of the maximum shear modulus G_{max} and the degradation of the secant shear modulus G/G_{max} and the increase of the hysteretic damping ξ with the amplitude of the cyclic shear strain γ_{cyc}. For a more thorough evaluation, the related curves of Vucetic & Dobry (1991) for a plasticity index PI = 0% are also added to this figure.

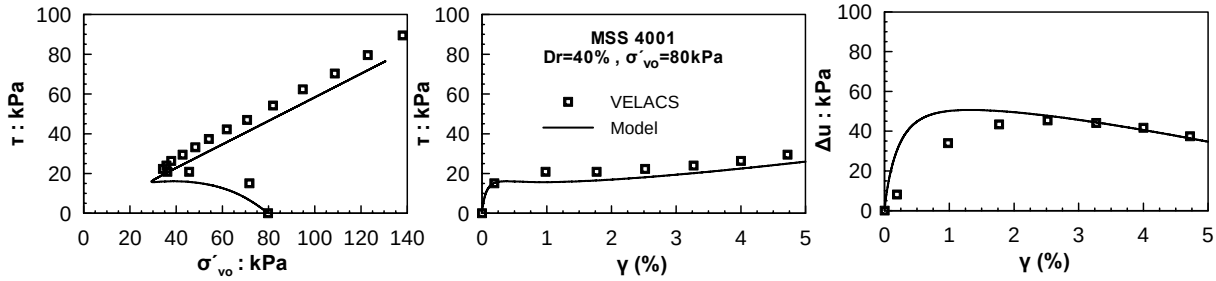

Figure 2. Comparison of simulation to data for a typical monotonic undrained simple shear test

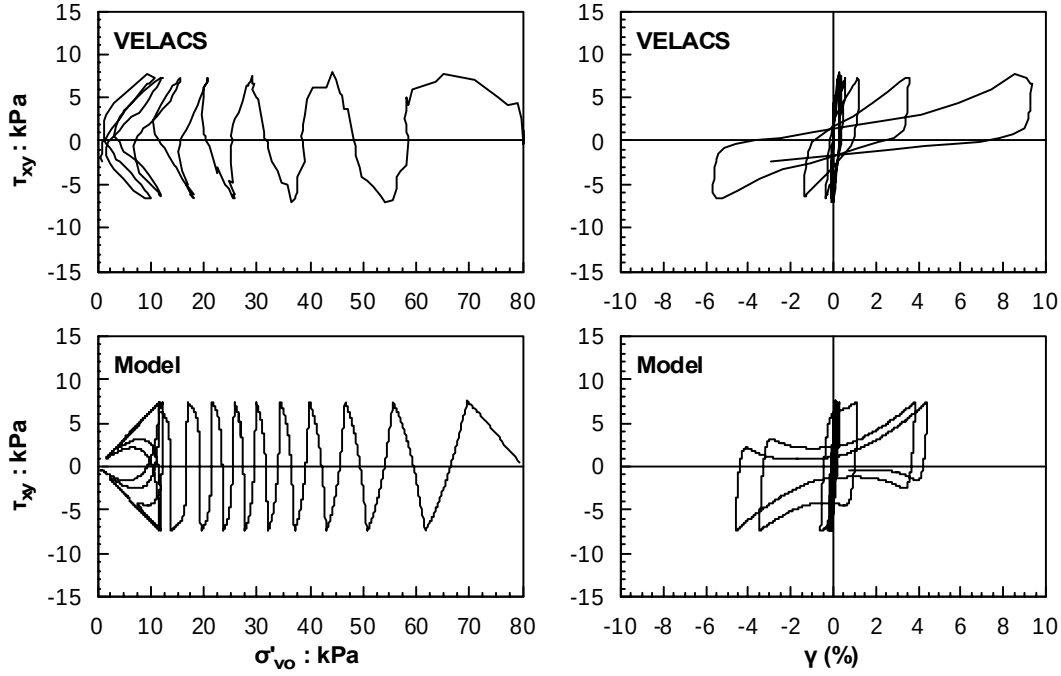

Figure 3. Comparison of simulation to data for a typical cyclic undrained simple shear test

More importantly, as described again in Papadimitriou et al. (2001), for the simulation of boundary value problems where the problem of earthquake loading is at hand and the soil is non-cohesive, one-to-one comparisons of selected liquefaction tests, like the one in Figure 3, may not portray the overall accuracy of the model for any cyclic stress ratio (CSR). Therefore, it is crucial that the model validation compares the liquefaction resistance curves of the data and the simulations, i.e. the curves that relate the CSR to the number of loading cycles N_L required for initial liquefaction. Hence, Figure 5 compares the liquefaction resistance curves from the available element tests, the respective simulations and related curves from the literature (DeAlba et al., 1976). Finally, the overall accuracy of the model simulations at large cyclic shear strain γ_{cyc} amplitudes should be established not only in terms of the number of cycles N_L to initial liquefaction, but also in terms of the rate of excess pore pressure Δu buildup in the cycles that precede initial liquefaction. An example of such an overall comparison is presented in Figure 6, where the excess pore pressure after the first (and most

significant) load cycle Δu_1 from all liquefaction tests is compared to the respective values from the simulations.

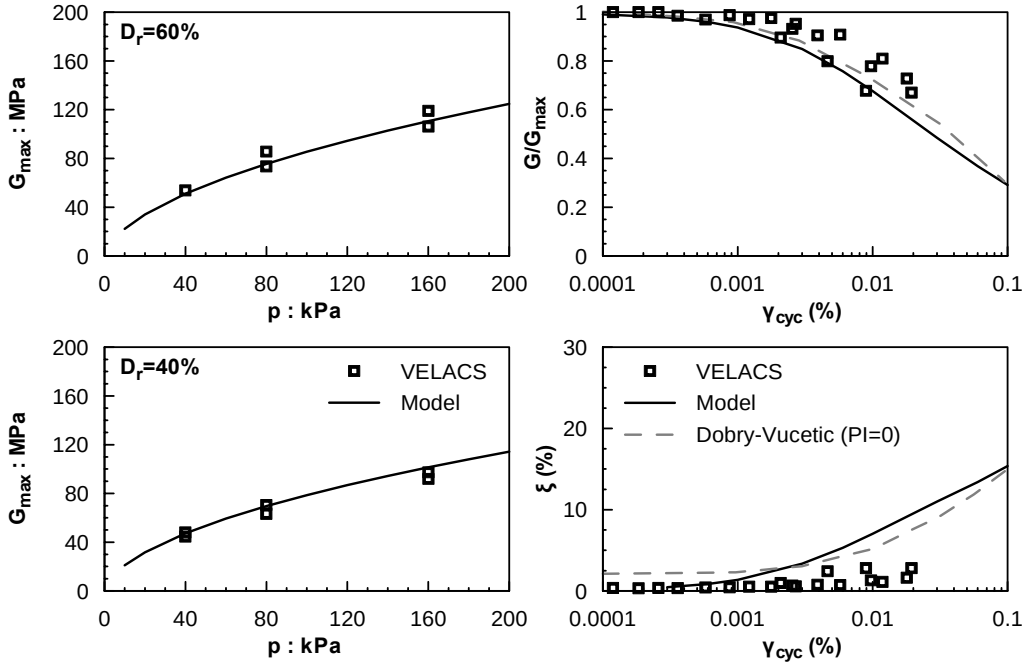

Figure 4. Summary comparison of simulations to data for cyclic shearing, in terms of the maximum shear modulus G_{max}, the secant shear modulus G/G_{max}-γ_{cyc} degradation curves and the damping ξ-γ_{cyc} increase curves

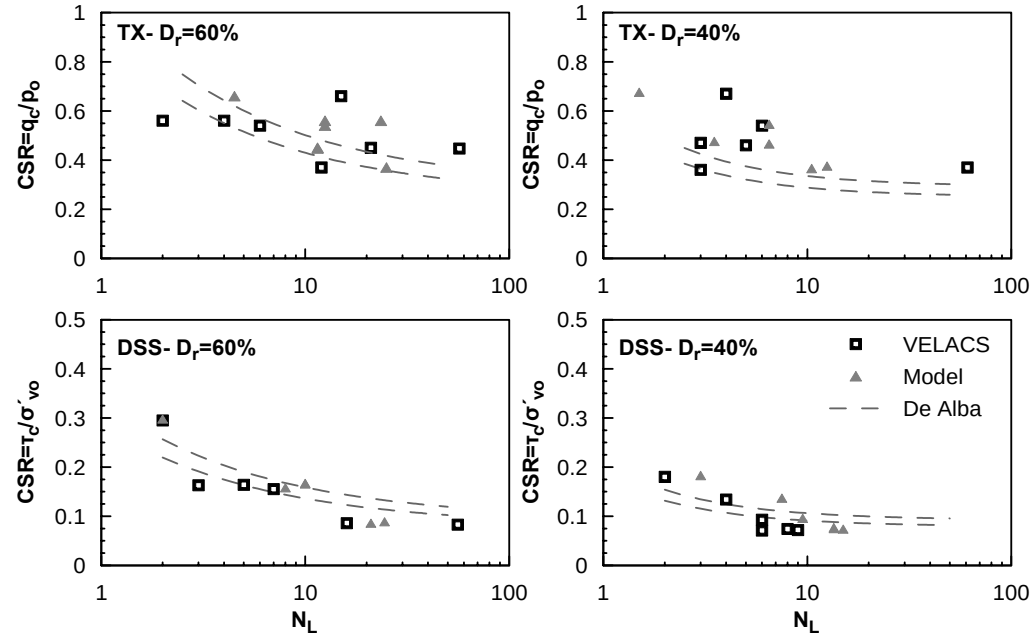

Figure 5. Summary comparisons of data to simulations for undrained cyclic shearing in terms of the number of cycles N_L for initial liquefaction

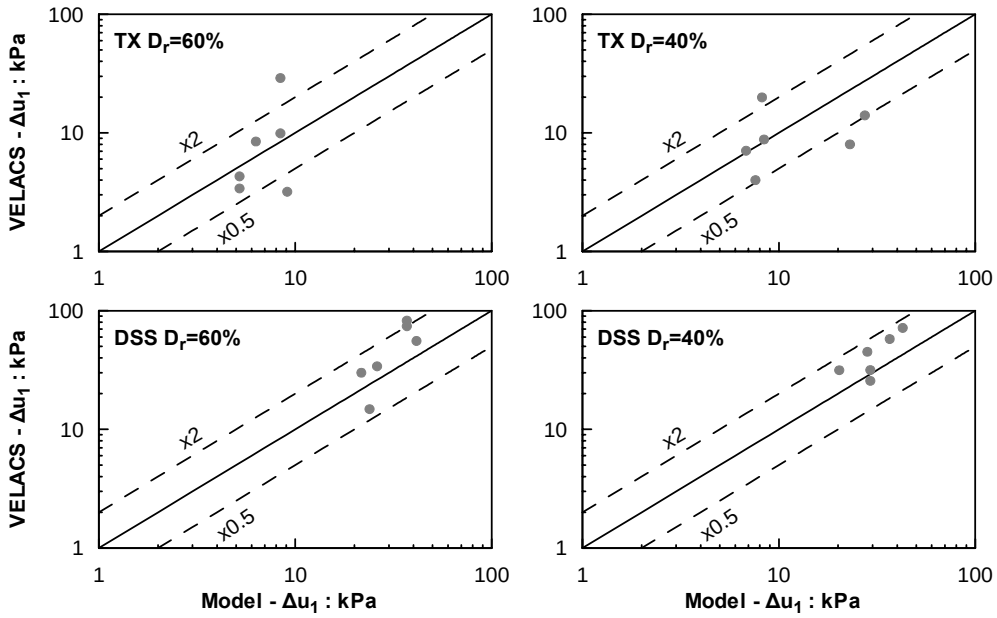

Figure 6. Summary comparison of data to simulations for cyclic shearing in terms of the excess pore pressure after the first load cycle Δu_1

VERIFICATION OF METHODOLOGY IN LIQUEFACTION-RELATED PROBLEMS

The proposed numerical methodology has been validated against results from the well-known VELACS experimental project (Arulmoli et al., 1992). In particular, results from Model tests No. 1 and No. 2 were used that simulate the one-dimensional (1D) response of a liquefiable soil layer under level and mildly sloping sites, respectively. Background reading for the liquefaction response of level and mildly sloping sites can be found in Youd and Idriss (2001) and Youd et al. (2002), respectively. In addition, model test No. 12 was used, which simulates the response of shallow foundations on liquefiable soils. Due to length limitations, this paper presents selected validation runs for the first two (2) model tests, which form the basis for any boundary value problem involving liquefaction. Documentation regarding the validation run of model test No. 12 can be found in Andrianopoulos et al. (2006a).

Horizontal Liquefiable Layer

The test arrangement and the instrumentation for Model test No. 1 is shown in Figure 7. In prototype scale, the experiment refers to a 10m deep Nevada Sand layer with 40% relative density, with the ground water surface at 1m above the ground surface. The centrifuge model was built inside a laminar box, which was tested at 50g centrifugal acceleration. The input motion consisted of twenty (20) more or less uniform cycles of horizontal acceleration with 0.235g amplitude and 2Hz frequency. The response of the level ground was monitored along the axis as well as closer to the box boundaries with eight (8) accelerometers, eight (8) pore pressure transducers and six (6) LVDTs measuring displacements. The grid used for the numerical analysis was uniform with 1.0m thick square elements. The horizontal acceleration time-history was applied at the bottom of the mesh, while the lateral boundaries were tied to one-another in order to ensure the same horizontal and vertical displacements of the two boundaries, as imposed by the laminar box device in the centrifuge test. The vertical acceleration during the experiments was minimal and was not taken into account during the simulation.

Figure 8 compares the time histories of the excess pore pressure ratio $r_u = \Delta_u/\sigma'_{vo}$ from the centrifuge test recordings to their numerically simulated counterparts, at various depths (-1.45m, -2.6m, -5.0m, -7.5m) of the sand layer, always along the axis of the centrifuge model. Both recordings and

simulations show initial liquefaction (r_u = 1.0) in the upper 5 – 7m. In particular, very high values of r_u develop from the first seconds of the shaking in the upper 2.5m, while deeper locations develop similarly high values of r_u at later stages of the shaking. Moreover, the rates of excess pore pressure buildup and dissipation are satisfactorily simulated, with the possible exception of the first 2 loading cycles during which the model shows more intense buildup than the data.

Figure 9 compares the time histories of ground acceleration (in percent of g) from the centrifuge test recordings to their numerically simulated counterparts, at the ground surface (AH3) and at the mid-depth (AH5 at a depth -5.0m) of the sand layer and along the axis of the centrifuge model. The agreement is satisfactory. It is especially noteworthy that the both the recording and the simulation depict a liquefaction-induced deamplification of the acceleration at the ground surface. More importantly, after t=5sec the extensive liquefaction of the ground nullifies the acceleration at the ground surface, as deduced by both the recording and the simulation. At the mid-depth of the sand layer, this deamplification is less intense in both simulation and recording, and especially the latter. The differences observed at this depth may be attributed to the relatively lower recorded vs simulated excess pore pressures from the depth of -5.0m and below.

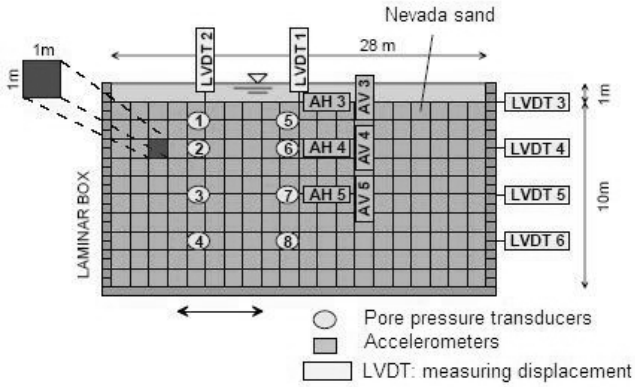

Figure 7. Schematic illustration of testing configuration of VELACS Model No.1

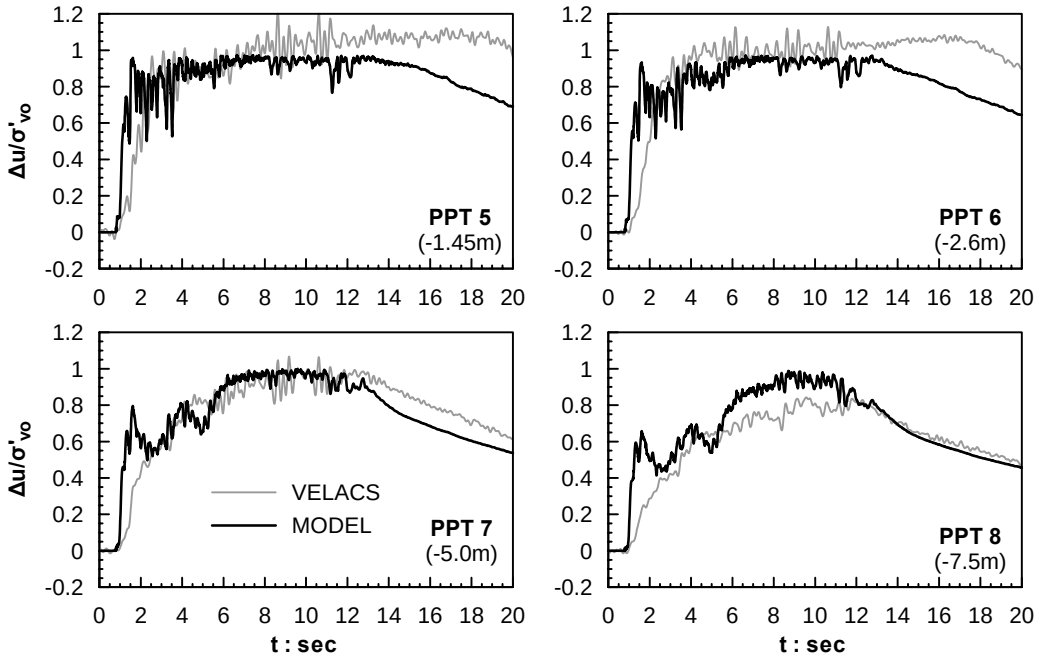

Figure 8. Comparison of data to simulations for the time history of the excess pore pressure ratio $\Delta u/\sigma'_{vo}$ developed at various depths along the axis of the model of the VELACS No.1 test

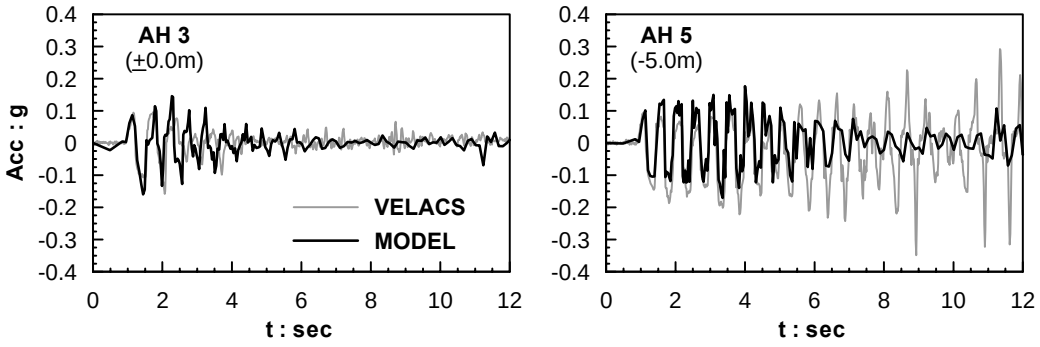

Figure 9. Comparison of data to simulations for the time history of ground acceleration developed at various depths along the axis of the model of the VELACS No.1 test

Mildly-Sloping Liquefiable Layer

The test arrangement and the instrumentation for Model test No. 2 is shown in Figure 10. In prototype scale, the experiment refers to a 10m deep Nevada Sand layer with 40% relative density. The centrifuge model was built inside a laminar box, which was tested at 50g centrifugal acceleration, and was tilted by 2^o in order to simulate lateral spreading conditions. The input motion consisted of twenty (20) more or less uniform cycles of horizontal acceleration with 0.235g amplitude and 2Hz frequency, the positive sign of which corresponds to the downslope direction (as is performed for the displacements, as well). The response of the mildly-sloping ground was monitored with ten (10) accelerometers, eight (8) pore pressure transducers and six (6) LVDTs measuring displacements. The grid used for the numerical analysis was uniform with 1.0m thick square elements. The horizontal acceleration time-history was applied at the bottom of the mesh, while the lateral boundaries were tied to one-another in order to ensure the same horizontal and vertical displacements of the two boundaries, as imposed by the laminar box device in the centrifuge test. The vertical acceleration during the experiments was minimal and was not taken into account during the numerical simulation

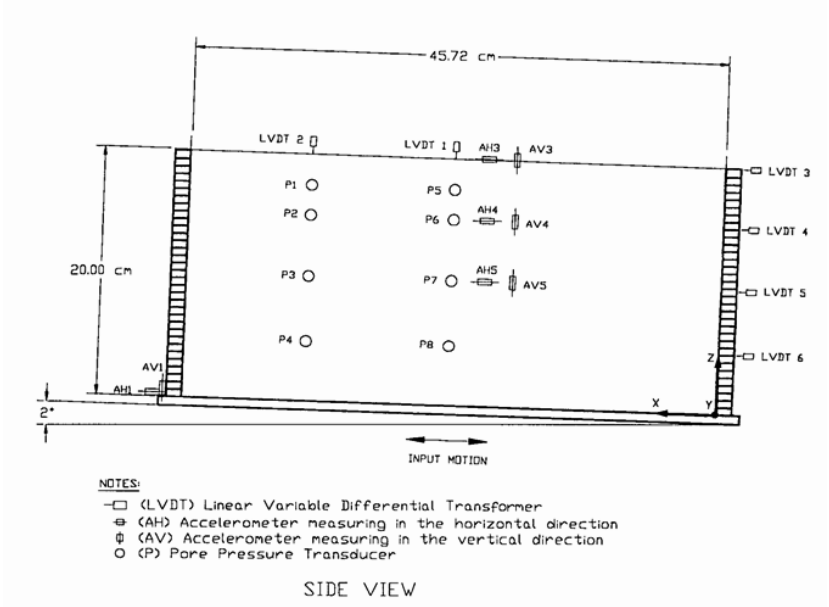

Figure 10. Schematic illustration of testing configuration of VELACS Model No.2

Figure 11 compares the time histories of the excess pore pressure ratio $r_u = \Delta_u/\sigma'_{vo}$ from the centrifuge test recordings to their numerically simulated counterparts, at various depths (-1.45m, -2.6m, -5.0m, -7.5m) of the sand layer and along the axis of the centrifuge model. As in the case of level ground conditions, both recordings and simulations show initial liquefaction ($r_u = 1.0$) in the upper 5m and smaller values of r_u at deeper locations. Again, very high values of r_u develop from the first seconds of

the shaking in the upper 2.5m, while deeper locations develop similarly high values of r_u at later stages of the shaking. The rates of excess pore pressure buildup and dissipation are satisfactority simulated, with the possible exception of the first 2 loading cycles during which the model shows more intense buildup than the data. Unlike the case of the level ground, the time histories of excess pore pressures show instant drops at the depths where initial liquefaction has been attained. This trait illustrates enhanced dilative response following a condition of $r_u \cong 1$ and is attributed to the shear stress offset originating from the static equilibrium of a mildly sloping ground.

Figure 12 compares the time histories of ground acceleration (in percent of g) from the centrifuge test recordings to their numerically simulated counterparts, at the ground surface (AH3) and at the mid-depth (AH5) of the sand layer, always along the axis of the centrifuge model. Satisfactory agreement is observed, since both the recording and the simulation show a liquefaction-induced deamplification of the acceleration at the ground surface (peak values of 0.10 – 0.12g, neglecting very high-frequency spikes), as compared to the 0.235g applied at the base. Unlike the case of the level ground, the acceleration does not nullify at the ground surface and this is attributed to the foregoing enhanced dilative respone and the thus induced lower excess pore pressures. Similarly, the accelerations from the recording and the simulation at mid-depth are again higher than their respective counterparts of the level ground case.

Figure 13 compares snapshots of the lateral displacements from the centrifuge test recordings to their numerically simulated counterparts at t = 3, 6, 9 and 12s. Similarly to what was measured in the centrifuge test, the simulation shows increased lateral displacements in the upper 5.0m, a fact attributed to the higher excess pore pressures and the ensuing lower shear strength of the upper layer. Close investigation of the results (in Figure 14) reveals an almost linear increase of the lateral displacement with time at any depth for the applied almost harmonic base excitation, an increase that is terminated at the end of shaking (at t=12sec). An index of the overall satisfactory simulation is that the final lateral displacement of the surface of the sand layer (LVDT3) was found equal to 42.7cm in the simulation and equal to 46.8cm in the centrifuge test, whereas at mid-depth the respective values are 19.4 and 14.3cm (LVDT5).

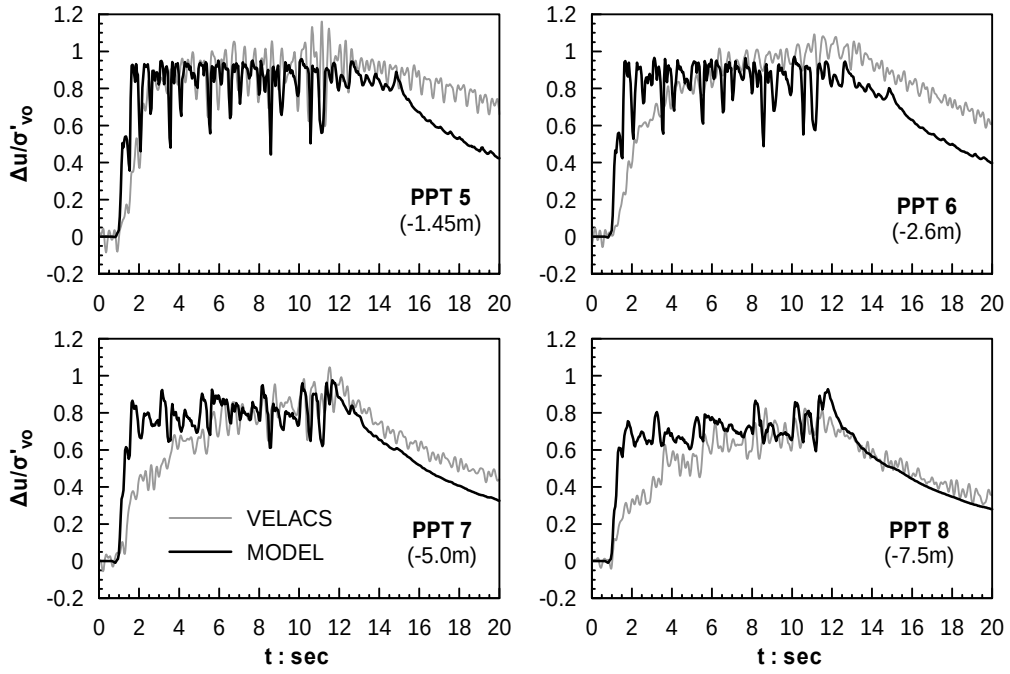

Figure 11. Comparison of data to simulations for the time history of the excess pore pressure ratio $\Delta u/\sigma'_{vo}$ developed at various depths along the axis of the model of the VELACS No.2 test

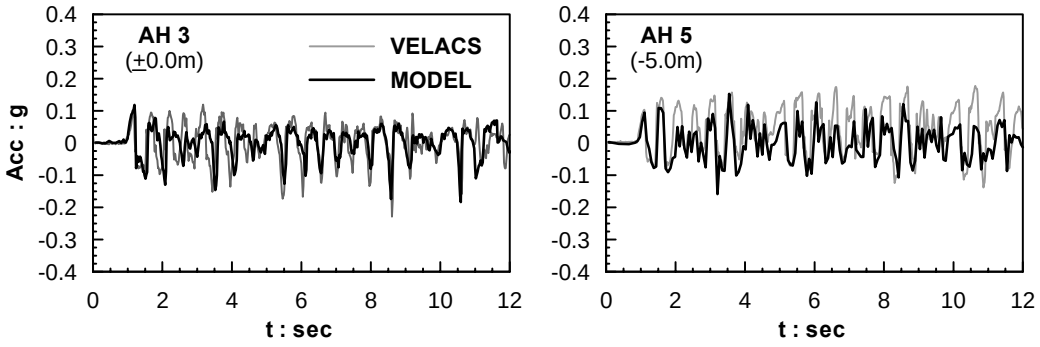

Figure 12. Comparison of data to simulations for the time history of ground acceleration developed at various depths along the axis of the model of the VELACS No.2 test

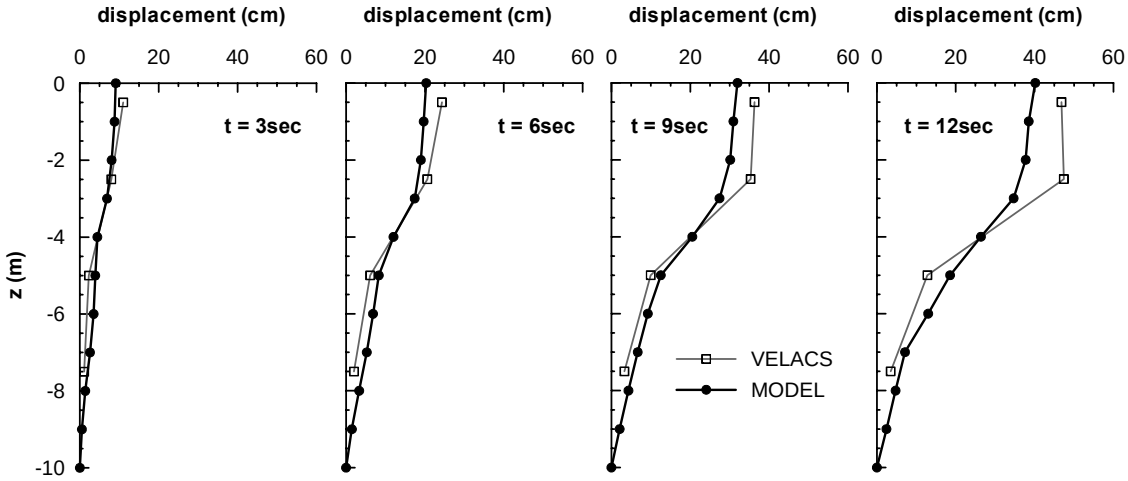

Figure 13. Snapshots of lateral displacement with depth at various instances of the shaking; comparison of data to simulations for the VELACS Model No.2

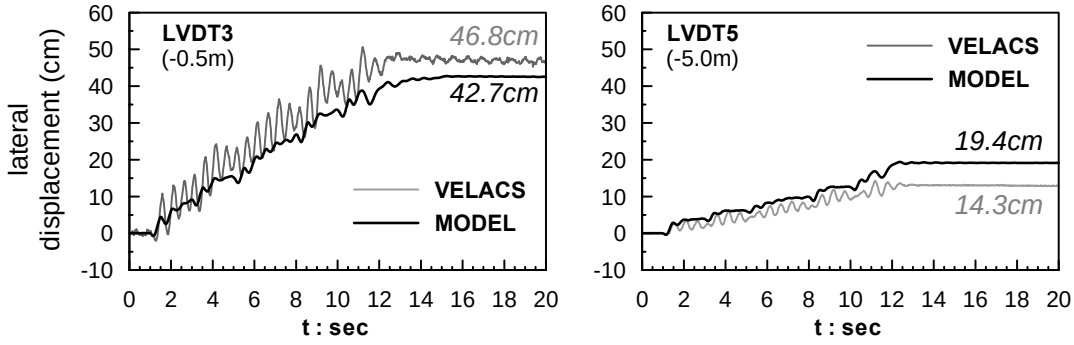

Figure 14. Comparison of data to simulations for the time history of lateral displacement developed at various depths of the model of the VELACS No.2 test

Further details from the foregoing comparisons can be found in Andrianopoulos (2006). What is of importance here is to underline that the ascertained level of accuracy in simulating VELACS Model tests No 1 and 2 was achieved with the same set of model constants, which were calibrated on the basis of laboratory element tests as shown in the previous paragraph. In addition, note that the proposed constitutive model, with the same set of model constants, has provided similar accuracy in simulation VELACS Model test No 12 (Andrianopoulos et al. 2006a).

In closing, given its accuracy, the proposed new numerical tool can be used for an in depth analysis of liquefaction-related phenomena. Of interest here is the mechanism of development of displacement in the lateral spreading phenomenon. The basis for this analysis is the simulation of the VELACS Model No 2. Of particular interest here are the effects of the enhanced dilative response following a condition of $r_u = 1$ that was observed in Figures 11 and 12 and was attributed to the shear stress offset originating from the static equilibrium of a mildly sloping ground. Hence, Figure 15 focuses on the time-histories of acceleration, velocity, excess pore pressure ratio at the ground surface and their relation to the respective time-histories of the lateral displacement at the ground surface, as well as the surface to base relative displacement. The shaded areas denote two sequential dilation spikes initiating at t=3.56sec and t=4.11sec. It is observed that the sharp dilation spikes (Fig 15b) correspond to acceleration pulses towards the upslope direction (negative sign in Fig 15a), which result in a decrease of the downslope velocity of the sand layer (positive sign in Fig 15a). As expected, the foregoing decrease of downslope velocity produces a reduction of the downslope displacement accumulation rate of the laterally spreading sand layer. Hence, during shaking, the accumulation of downslope displacement (attributed to the reduced shear strength produced from very high r_u values near liquefaction) is temporarily obstructed by successive dilation spikes (see Fig 15c), that may even lead to temporary upslope movement if the shaking is strong enough. Interestingly, the successive dilation spikes have a period of T = 0.56sec, i.e. the elongated period of the applied motion of 2Hz. Hence, the accumulation of displacement due to lateral spreading is remniscent of a "stick-slip" physical mechanism, with a return period that is somewhat larger than the predominant period of the applied seismic excitation. This period elongation of the motion is obviously attributed to the reduction of the dynamic properties of the sand due to liquefaction.

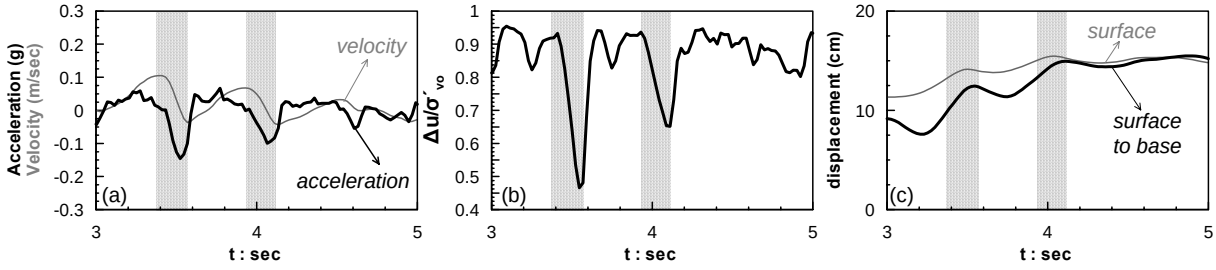

Figure 15. Detail of time-histories of acceleration, velocity, excess pore pressures and lateral displacement from the simulation of the VELACS No.2 test

CONCLUSIONS

On the basis of the comparisons with test data from element and centrifuge tests on the same Nevada sans, it may be concluded that the proposed constitutive model predicts with accuracy the stress-strain response of non-cohesive soils (sands and silts) during loading:

- at element level, as well as in complex boundary value problems,
- for monotonic and cyclic conditions,
- under small, medium and large strain amplitudes,
- under drained and undrained conditions, and
- for any initial soil density, stress level and loading direction.

From a practical point of view, the most important asset of the proposed methodology is that for all aforementioned conditions, a single soil-specific set of model constants is needed.

Furthermore, it has been shown that the proposed implemented UDM in *FLAC* is a promising numerical tool for performing realistic, fully-coupled dynamic analyses for practical problems of Earthquake Geotechnical Engineering. As such, it can be readily used for the in depth study of very complicated problems. In particular, this paper showed that the accumulation of displacement due to

lateral spreading is remniscent of a "stick-slip" physical mechanism, with a return period that is somewhat larger than the predominant period of the applied seismic excitation.

ACKNOWLEDGEMENTS

The work presented herein has been financially supported by the General Secretariat for Research and Technology (Γ.Γ.Ε.Τ.) of Greece, through research project ΕΠΑΝ – ΔΠ23 ("X-SOILS"). This contribution is gratefully acknowledged.

REFERENCES

Andrianopoulos, K.I., "Numerical modeling of static and dynamic behavior of elastoplastic soils", *Doctorate Thesis*, Department of Geotechnical Engineering, School of Civil Engineering, National Technical University of Athens (in Greek), 2006

Andrianopoulos, K.I., Papadimitriou, A.G. and Bouckovalas, G.D., "Bounding surface models of sands: Pitfalls of mapping rules for cyclic loading", *Proceedings, 11th International Conference on Computer Methods and Advances in Geomechanics*, Torino, June, Vol. 1: 241-248, 2005

Andrianopoulos, K.I., Bouckovalas, G.D., Karamitros D.K., Papadimitriou, A.G., "Effective stress analyses for the seismic response of shallow foundations on liquefiable sand", *Proceedings, 6th European Conference on Numerical Methods in Geotechnical Engineering*, Graz, September, 2006

Andrianopoulos, K.I., Papadimitriou, A.G., Bouckovalas, G.D., "Implementation of a bounding surface model for seismic response of sands", *Proceedings, 4th International FLAC Symposium on Numerical Modeling in Geomechanics*, May, 2006

Arulmoli, K., Muraleetharan, K.K., Hossain, M.M. and Fruth, L.S., "VELACS: verification of liquefaction analyses by centrifuge studies; Laboratory Testing Program – Soil Data Report", *Research Report*, The Earth Technology Corporation, 1992

Been, K. & Jefferies, M.G., "A state parameter for sands", *Geotechnique*, 35, no.2, 99-112, 1985

Dafalias, Y.F. and Manzari, M.T. "Simple plasticity sand model accounting for fabric change effects", Journal of Engineering Mechanics, ASCE, 130(6): 622-634, 2004

Elgamal A., Yang Z., Parra E., "Computational modeling of cyclic mobility and post-liquefaction site response", *Soil Dynamics and Earthquake Engineering,* 22 (4), 259-271, 2002

Itasca Consulting Group, Inc., "FLAC – Fast Lagrangian Analysis of Continua", Version 3.4, *User's Manual*, Minneapolis: Itasca, 1998

Manzari, M.T. and Dafalias, Y.F., "A critical state two-surface plasticity model for sands", Geotechnique, 47(2): 255-272, 1997

Naylor, D.J., "A continuous plasticity version of the critical state model", *International Journal of Numerical Methods in Engineering*, 21: 1187-1204, 1985

Papadimitriou, A.G., Bouckovalas, G.D. and Dafalias, Y.F., "Plasticity model for sand under small and large cyclic strains", *Journal of Geotechnical and Geoenvironmental Engineering*, ASCE, 127, no. 11, 973-983, 2001

Papadimitriou, A.G. and Bouckovalas, G.D., "Plasticity model for sand under small and large cyclic strains: a multiaxial formulation", *Soil Dynamics and Earthquake Engineering*, 22, 191-204, 2002

Sloan, S.W., Abbo A. J. and Sheng D., "Refined explicit integration of elastoplastic models with automatic error control", *Engineering Computations,* 18 (1/2), 121-154, 2001

Youd, T.L. and Idriss, I.M., "Liquefaction resistance of soils: Summary report from the 1996 NCEER/NSF workshops on evaluation of liquefaction resistance of soils", *Journal of Geotechnical and Geoenvironmental Engineering*, ASCE, 127(4): 297-313, 2001

Youd, T.L., Hansen, C.M. and Bartlett, S.F., "Revised multilinear regression equations for prediction of lateral spread displacement", *Journal of Geotechnical and Geoenvironmental Engineering*, ASCE, 128(12): 1007-1017, 2002